



Observational benchmarks inform representation of soil organic carbon dynamics in land surface models

Kamal Nyaupane¹, Umakant Mishra^{2*}, Feng Tao³, Kyongmin Yeo⁴, William J. Riley⁵, Forrest M. Hoffman⁶ and Sagar Gautam²

¹Environmental science and Engineering Program, The University of Texas at El Paso, El Paso, TX 79968, United States.

² Biomaterials & Biomanufacturing, Sandia National Laboratories, Livermore, CA, 94550, United States.

³Ministry of Education Key Laboratory for Earth System Modelling, Department of Earth System Science, Tsinghua University, Beijing, 100084, China

⁴IBM Thomas J. Watson Research Center, Yorktown Heights, NY, 10562, United States.

⁵Earth & Environmental Sciences, Lawrence Berkeley National Laboratory, Berkeley, CA, 94720, United States.

⁶Climate Change Institute, Oak Ridge National Laboratory, Oak Ridge, TN, 37830, United States.

*Corresponding author Email: umishra@sandia.gov



1 **Abstract**

2 Representing soil organic carbon (SOC) dynamics in Earth system models (ESMs) is a key
3 source of uncertainty in predicting carbon climate feedbacks. Machine learning models can help
4 identify dominant environmental controllers and their functional relationships with SOC stocks.
5 The resulting knowledge can be implemented in ESMs to reduce uncertainty and better predict
6 SOC dynamics over space and time. In this study, we used a large number of SOC field
7 observations ($n = 54,000$), geospatial datasets of environmental factors ($n = 46$), and two
8 machine learning approaches (Random Forest (RF) and Generalized Additive Modeling (GAM))
9 to: (1) identify dominant environmental controllers of global and biome-specific SOC stocks, (2)
10 derive functional relationships between environmental controllers and SOC stocks, and (3)
11 compare the identified environmental controllers and predictive relationships with those in
12 Coupled Model Intercomparison Project phase six (CMIP6) models. Our results showed that
13 diurnal temperature, drought index, cation exchange capacity, and precipitation were important
14 observed environmental controllers of SOC stocks. RF model predictions of global-scale SOC
15 stocks were relatively accurate ($R^2 = 0.61$, $RMSE = 0.46 \text{ kg m}^{-2}$). In contrast, precipitation,
16 temperature, and net primary productivity explained $>96\%$ of ESM-modeled SOC stock
17 variability. We also found very different functional relationships between environmental factors
18 and SOC stocks in observations and ESMs. SOC predictions in ESMs may be improved
19 significantly by including additional environmental controls (e.g., cation exchange capacity) and
20 representing the functional relationships of environmental controllers consistent with
21 observations.

22



23 **Keywords:** Environmental controllers, Earth system models, soil organic carbon, net primary
24 productivity, machine learning, model benchmarking

25

26 **1. Introduction**

27 Soil is the largest actively cycling carbon pool in terrestrial ecosystems and stores almost twice
28 the amount of carbon as in the current atmosphere (Lal, 2016). A small change in soil carbon
29 stocks can lead to large changes in the atmospheric CO₂ concentration and future climate change
30 trajectories. Soils also play a crucial role in sequestering atmospheric CO₂ as soil organic carbon
31 (SOC) (Hinge et al., 2018). Thus, sequestration, protection, and sustainable management of SOC
32 stocks can be a promising climate mitigation strategy (Lal, 2020). Accurate representation of
33 global SOC storage and its environmental controllers are essential for predicting realistic
34 changes of SOC under different land use and climate change scenarios. Yet, no consensus exists
35 among current Earth system models (ESMs) in representing the spatial distributions of global
36 SOC storage and its fate under future climate change scenarios (Friedlingstein et al., 2014.;
37 Arora et al., 2020).

38 Multiple environmental variables, including climatic and topographic factors, land use history,
39 and edaphic properties, have been identified as possible controllers of SOC storage (Georgiou et
40 al., 2021; Mishra et al., 2022). Current ESMs, however, use the effects of only a limited number
41 of environmental factors in representing SOC storage and dynamics. A recent study that
42 compared SOC stocks from multiple ESMs against observations indicated a large knowledge gap
43 in both ESMs and observations (Georgiou et al., 2021). Therefore, it is important to compare
44 ESM simulations against global SOC observational datasets to evaluate model performance and
45 identify key environmental controllers of global SOC storage.



46 Benchmarking ESM simulations with observed data is a common approach for model evaluation
47 (Luo et al., 2012; Todd-Brown et al., 2013; Collier et al., 2018). Through comparing model
48 simulations with observations, model strengths, deficiencies, and needed improvements can be
49 identified. The resulting understanding from SOC benchmarking could lead to new ESM land
50 model structures (by identifying key processes) and new parameterizations (by quantifying key
51 relationships between SOC and environmental variables). Thus, benchmarking analysis of ESMs
52 is an effective tool to reduce uncertainties in predicting SOC dynamics and can provide more
53 realistic information for managing SOC under changing climate conditions (Lauer et al., 2017).
54 Currently ESMs predict SOC stocks primarily with model representations that depend on soil
55 temperature, moisture, and belowground net primary production (Todd-Brown et al., 2013).
56 ESMs capture the positive correlation between NPP and precipitation, resulting in high SOC
57 stocks for areas with high NPP in moist regions (Sun et al., 2016). Higher temperature increases
58 soil respiration, which, in the short-term, reduces SOC storage. In the longer-term, increased soil
59 respiration can release nutrients, leading to increased plant growth, belowground carbon inputs,
60 and thereby SOC stocks; the balance of these factors can take centuries to manifest (Mekonnen
61 et al., 2022). Soil respiration temperature sensitivity is often defined based on Q_{10} or Arrhenius
62 equations in ESMs (Wynn et al., 2006), although low- and high-temperature modifications to
63 these relationships are likely needed (Jiang et al., 2013; Azizi-Rad et al., 2022).
64 In a previous U.S. continental-scale study, we derived empirical non-linear relationships between
65 SOC and environmental factors that produced comparable prediction accuracy to a random forest
66 (RF) machine learning approach (Mishra et al., 2022). We apply a similar approach in this study
67 in both global field observations and ESMs to (1) identify key observed environmental controllers
68 of, and functional relationships with, global SOC stocks and (2) evaluate ESMs with these



69 observational benchmarks. Simulated SOC stocks from three CMIP6 ESMs (i.e., Community
70 Earth System Model (CESM, Hurrell et al., 2013); U.K. Earth System Model (UKESM, Sellar et
71 al., 2019); Beijing Climate Center model (BCC, Xiao-Ge et al., 2019) were benchmarked with
72 50,000 SOC profile observations across the globe. We used a machine learning (i.e., random
73 forest) approach with 46 environmental factors to identify the key environmental controllers of
74 SOC stocks at the global scale. We then applied a generalized additive model (GAM) to derive the
75 predictive relationships between these key environmental factors and SOC stocks in observations
76 and ESM simulations. Specific objectives of this study were to: (1) identify dominant
77 environmental controllers of SOC stocks in field observations and CMIP6 ESMs, (2) derive
78 observed and ESM-modeled functional relationships between environmental factors and SOC
79 stocks, and (3) analyze these functional relationships to inform needed improvements in ESM
80 representations of SOC dynamics.

81 **2. Materials and Methods**

82

83 ***2.1 Soil organic carbon stock observations***

84

85 We used two datasets of SOC stocks for the topsoil layer (i.e., 0 – 30 cm) and the whole soil profile
86 (i.e., 0 – 100 cm). The World Soil Information Service (WoSIS) compiled SOC profiles across the
87 globe after quality assessment. The 2019 snapshot of the WoSIS dataset contained 111,380 soil
88 profiles with SOC content information (unit: g C g-soil⁻¹) at different soil depths (Batjes et al.,
89 2020). We estimated the SOC stock (g C m⁻²) at different soil layers using:

$$90 \quad SOC \text{ Stock} = SOC \text{ Content} \times \left(1 - \frac{G}{100}\right) \times BD \times D \quad (1)$$

91 where G is the coarse fragment fraction (%); BD is the bulk density of soil (g m⁻³); and D is the
92 soil layer depth (m).



93 When the measured bulk density value was absent from the dataset, we used a pedo-transfer
94 function (Yigini et al., 2018) to estimate the soil bulk density:

$$95 \quad BD = \alpha + \beta \times \exp(-\gamma \times OM) \quad (2)$$

96 Where OM is organic matter, equivalent to $SOC \times 1.724$, with SOC content in percent (%); α , β ,
97 and γ are fitting parameters. We found $\alpha = 0.32$, $\beta = 1.30$, and $\gamma = 0.0089$ after fitting WoSIS data
98 to this equation.

99 Another dataset we used in this study was compiled from Mishra et al. (2021). This dataset
100 contained 2,546 soil profiles with SOC stock (g C m^{-3}) information from permafrost regions in
101 North America, northern Eurasia, and the Qinghai-Tibet Plateau. In total, we used 113,926 soil
102 profile observations from these two data sources. SOC stocks of different soil layers were then
103 summed to SOC stocks in 0 – 30 cm and 0 – 100 cm depth intervals. Because not all these soil
104 profiles covered the whole 0 – 30 cm or 0 – 100 cm intervals, we used a total of 54,000 soil profiles
105 that included SOC stock information for both depth intervals. The geographical distributions of
106 soil profiles used in this study are shown in Figure 1. Because SOC stock values across the globe
107 were highly skewed, we used a natural logarithm transformation in this study.

108

109 *2.2 Environmental predictors of SOC stocks*

110

111 The storage and cycling of SOC are controlled by multiple environmental factors. In this study,
112 we used observations of 46 environmental variables, which represented major soil forming factors
113 (McBratney et al., 2003.). Twenty-one of the 46 environmental variables were climatic variables,
114 including annual average temperature, precipitation, evapotranspiration, drought severity index,
115 and statistics for different temporal scales (e.g., during the wettest and driest quarter in a year).
116 Thirteen of the 46 variables described soil properties (e.g., clay content, sand content, silt content,
117 soil texture, pH, and cation exchange capacity). Six variables represented topographic factors (e.g.,



118 elevation and soil depth). Six variables represented land use and land cover types. All the
119 categorical variables were converted to integer variables and the environmental variables were
120 resampled to a common 1 km resolution. The environmental factors, their original spatial
121 resolution, and data sources are provided in the supporting information (Table S1).

122

123 *2.3 Selection of dominant environmental controllers of SOC stocks*

124

125 We used RF to select dominant environmental predictors of SOC stocks within biomes and at
126 global scale in both observations and ESMs. RF is an ensemble learning method, which is an
127 extension of the classical Classification and Regression Trees (CART). Building a collection of
128 uncorrelated CARTs through bootstrapping the samples and applying the random subspace method
129 at each branch of the trees, RF improves the prediction performance (Breiman, 2001; Wiesmeier
130 et al., 2011; Mishra et al., 2020). RF is well known for its strength in modeling highly nonlinear
131 relationships between the predictors and is robust to overfitting (Chagas et al., 2016). Moreover,
132 RF is not very sensitive to the choice of the hyperparameters, which makes RF one of the most
133 popular off-the-shelf model for many classification and regression problems.

134 In this study, we trained the RF model using SOC content as a response variable and environmental
135 factors as predictors. The model performance was evaluated using the coefficient of determination
136 (R^2) and root mean square error (RMSE). A 10-fold cross-validation was used to compute R^2 and
137 RMSE. Biome-specific analyses were conducted on a subset of the global dataset. For biome
138 classification, we used the IGBP land classes (Loveland and Belward, 1997). The “Random-
139 Forest” package in R was used to train a RF model using all the observed environmental factors in
140 the dataset and to identify dominant environmental controllers of SOC stocks. Prior to fitting into
141 the final model, we performed a potential collinearity test among the environmental variables by



142 calculating pairwise correlations and variance influence factors. Predictors showing a variance
143 influence factor (VIF) value greater than 10 were omitted, leaving 14 uncorrelated environmental
144 predictors of SOC stocks in the observations.

145

146 ***2.4 Generalized additive model***

147

148 Generalized additive model (GAM) is an extension of generalized linear models, which employs
149 spline functions to model nonlinear relationships between predictor and response variables (Arnold
150 et al., 2013). In GAM, the relationship between predictor and response variable can be modeled as
151 (Hastie and Tibshirani, 1987):

$$152 Y = C + \sum_{i=1}^p f_i(X_i) \quad (3)$$

153 Here, Y is the response variable (SOC), C is a constant, X_i are the environmental controller
154 variables, f_i is a spline function for X_i, and p is the total number of environmental controllers. We
155 used the “mgcv” package in R to build GAMs for the observations as well as CMIP6 ESMs
156 (Arnold et al., 2013). The performance of GAMs was evaluated by using R² and RMSE.

157

158 ***2.5 Earth system model outputs***

159

160 We downloaded and aggregated the SOC and environmental controller data from three ESMs that
161 participated in CMIP6: Community Earth System Model (Hurrell et al., 2013.), U.K. Earth System
162 Model (Sellar et al., 2019), and Beijing Climate Center model (Xiao-Ge et al., 2019). These ESMs
163 included most of the environmental factors used by CMIP6 ESMs. ESMs did not report depth-
164 dependent soil carbon projections, making direct comparison with depth-dependent SOC
165 observations difficult. The majority of land models used in ESMs were designed to simulate topsoil



166 carbon for topsoil depth; thus, we assumed that the simulated soil carbon is contained within 1 m
167 of soil profile to simplify comparison with observations.

168

169 3. Results

170

171 3.1 Descriptive statistics of SOC observations

172

173 The average global SOC stock in the 0 - 1 m depth interval was 13.5 kg C m^{-2} , ranging from 0.14-
174 $435.3 \text{ kg C m}^{-2}$. Summary statistics of SOC stocks at global scale and within different biomes is
175 presented in Table 1. The standard deviation showed a similar spread in SOC stock values in
176 croplands ($n=21820$), savannas ($n=9807$) and grasslands ($n=5938$). However, in forests ($n=12164$)
177 and shrublands ($n=3769$), the standard deviation was higher indicating a large range in SOC stock
178 values. Distributions of total SOC stocks in different biomes are presented in Figure 2. Across
179 different biomes, forests contain the largest organic carbon content globally, with a mean value of
180 15.9 kg C m^{-2} and standard deviation 20.7 kg C m^{-2} .

181

182 3.2 Dominant environmental controllers of SOC stocks in observations and ESMs

183

184 At the global scale, we found that diurnal temperature, drought severity index, annual
185 temperature, and cation exchange capacity are the dominant environmental controllers of SOC
186 stocks in observations (Figure 3). By including all the environmental controllers, the RF model
187 explained 61% of observed global spatial SOC variation. R^2 ranged from 48% in savannas to
188 65% in croplands (Table 2) and the importance of key environmental controllers varied between
189 biomes (Figure 4). In croplands, precipitation, drought, diurnal temperature, and cation exchange
190 capacity were identified as the dominant controllers of SOC stocks. In grasslands, annual
191 temperature, cation exchange capacity, and sand content were the dominant controllers. In
192 forests, cation exchange capacity, precipitation, and temperature were dominant controllers. In



193 shrublands, annual temperature, soil pH, and cation exchange capacity were the most important
194 controllers. In savannas, soil related variables, temperature, and precipitation were the most
195 important controllers. Across all land cover types, we found that cation exchange capacity and
196 seasonal climatic variables were the dominant environmental controllers of SOC stocks.

197 In contrast, the RF model with 8 environmental variable predictors made near-perfect
198 predictions of ESM simulated SOC stocks (average $R^2 = 0.95$, R^2 values for UKESM, CESM,
199 and BCC model were 0.99, 0.89, and 0.98, respectively). In contrast to the results obtained from
200 the observed SOC stocks, the dominant controllers of ESM simulated SOC stocks were annual
201 temperature, net primary productivity (NPP), and annual precipitation (Figure 5). In particular,
202 NPP was by far the most dominant predictor of SOC stocks in the UKESM.

203

204 ***3.2 Predictive relationships between environmental factors and SOC stocks***

205 Dominant environmental controllers of observed SOC stocks identified by the RF model
206 were used in GAM to derive predictive relationships. We retrieved explicit analytical
207 expressions by fitting the splines derived from GAM in the observation dataset. Notwithstanding
208 its role as the sole carbon source to soil, our results did not show NPP as a strong controller on
209 observed SOC stocks (Figure 6a). In contrast with field observations, all ESMs showed
210 significant dependence (exponential increase) of SOC stocks on NPP. Our results also showed
211 that observed SOC stocks increased almost linearly with observed annual precipitation (Figure
212 6b). In contrast, ESMs show different relationships between SOC and precipitation. We found a
213 nonlinearly increasing SOC with precipitation in CESM, an initial sharply increasing and then
214 decreasing relationship in UKESM, and a decreasing relationship in BCC ESM. On the
215 relationship between SOC storage and soil texture and elevation, ESMs do not capture the



216 observed relationships. Our results indicated that observed SOC stocks decreased with clay
217 content in the interval between 0 and 20%, and then increased with clay content above 20%
218 (Figure 6c). Observed SOC stocks increased with silt content up to 55% and then decreased
219 (Figure 6d).

220 SOC stock functional relationships differed between the three ESMs and in many cases
221 differed with the relationships we derived from observations. In terms of the effects of annual
222 temperature on modeled SOC storage, we found that SOC stocks decreased with annual
223 temperature and were most sensitive to temperature in the range between 0 and 10°C (Figure 6e).
224 However, while the three ESMs captured the general negative relationship between SOC storage
225 and temperature, none of them correctly described the varying sensitivity of SOC in different
226 temperature ranges (especially in extreme temperature ranges <0°C and >20°C). In representing
227 the control of elevation on SOC storage, only UKESM showed consistent patterns with
228 observations, where SOC storage remained stable when the elevation was lower than 2000 m and
229 decreased when the elevation was higher than 2000 m (Figure 6f).

230

231 **Discussion**

232 Previous studies have suggested that the spatial variation of SOC is dependent on multiple
233 environmental factors such as climatic and edaphic variables, geography, and vegetation. Here,
234 we found that climatic variables (i.e., temperature and precipitation) are the most important
235 controllers of global SOC stocks, followed by edaphic variables (i.e., cation exchange capacity),
236 topography (i.e., elevation), and vegetation (i.e., NPP). Using boosted regression trees, Luo et al.
237 (2021) studied edaphic and climatic controls on SOC dynamics at different soil depths and found
238 that soil type and climatic variables are the most important variables in explaining the SOC



239 stocks (Luo et al., 2021). In this study, we found that seasonal climatic variables such as diurnal
240 temperature range and precipitation seasonality are among the most important environmental
241 controllers in explaining the spatial variation of SOC stocks. This result indicates the critical role
242 of seasonal and interannual climatic variables in understanding SOC dynamics.

243 The importance of climatic variables on global SOC storage emerges from close links
244 with processes that affect ecosystem productivity and soil microbial processes. Consistent with
245 our findings, Wiesmeier et al. (2014) reported climatic variables (temperature and precipitation)
246 as significant controllers of SOC stocks up to 1 m depth in German soils under oceanic climate
247 (Wiesmeier et al., 2014). Sreenivas et al. (2014) used RF to predict the SOC variability across
248 semi-arid and humid areas of India in the top 30 cm of soil and found that the top three
249 environmental controllers were land cover, mean temperature of hottest months, and mean
250 annual precipitation (Sreenivas et al., 2016). In our analysis, the overall relative importance of
251 climatic variables was significantly higher than other variables at the global and biome scales.

252 Soil properties were identified as the second most important controllers of global SOC
253 stocks. Soil properties impact various processes that govern soil carbon dynamics. For example,
254 soil properties impact microbial activity, porosity, and oxygen availability in the soil profile,
255 which directly or indirectly control soil water dynamics, plant growth, and SOC stocks.
256 Consistent with our findings, Luo et al. (2021) reported that sand content, silt content, and soil
257 pH were significant controllers of SOC stocks in all soil depths globally.

258 The Palmer drought severity index, which indicates low soil moisture availability, was a
259 dominant controller of global SOC stocks. Consistent with our findings, Li et al. (2021) reported
260 that soil particle size and soil water content were the most influential predictors of SOC variation
261 (Li et al., 2021). Soil drought, indicating more negative soil water potential and low soil



262 hydraulic conductivity, can cause tree mortality (Anderegg et al., 2012). Climate extremes like
263 droughts can impact the structure, composition, and functioning of terrestrial ecosystems and can
264 thereby severely affect the regional carbon cycle (Frank et al., 2015).

265 Cation exchange capacity is a soil property that indicates the active soil surface to which
266 SOC may be adsorbed, and polyvalent metal cations can play a significant role in SOC
267 stabilization by binding organic compounds to mineral surfaces (O'Brien et al., 2015; Solly et
268 al., 2020). O'Brien et al., (2015) found that exchangeable soil Ca^{2+} is a significant predictor of
269 SOC stocks. This relationship is supported by the mechanism that Ca^{2+} and Mg^{2+} promote clay
270 flocculation and bind organic matter to clay surfaces. Solly et al. (2020) reported that SOC and
271 cation exchange capacity are significantly related in both topsoil and subsoil with strong positive
272 relationship.

273 After climatic factors and cation exchange capacity, topography and vegetation (NPP)
274 were important controllers of observed global SOC stocks. Effects of NPP on observed SOC
275 stocks was found to be small (~6% in 0-100 cm soil depth). Similar to our findings, Luo et al.
276 (2021) reported NPP explaining about 10% of the variation of SOC stocks. NPP delivers the
277 primary inputs of carbon to soil and NPP generally increases with moisture, temperature, and
278 CO_2 up to a certain limit (Todd-Brown et al., 2013). NPP also depends on the availability of soil
279 nutrients. Most ESMs overestimate the increase in SOC pools in response to NPP increases
280 (Todd-Brown et al., 2013). The effects of NPP on SOC also depend on biome type and soil
281 depths (Luo et al., n.d.; Georgiou et al., 2021). The contribution of NPP on SOC stocks mostly
282 depends on how much NPP ends up in the soil and how it is translocated to different soil depths.
283 Georgiou et al. (2021) reported a saturating relationship of SOC stocks with increasing NPP in a



284 global observational dataset. However, Chen et al., (2018) reported high SOC stocks with
285 increasing productivity and soil water holding capacity (Chen et al., 2018).

286 The three CMIP6 ESMs we analyzed predicted SOC stocks mostly as a function of
287 temperature, precipitation, and NPP. These ESMs simulated positive correlations between SOC
288 stocks and NPP (Figure 5a), resulting in high SOC stocks in areas with high NPP in most regions
289 (Shi et al., 2013; Sun et al., 2016). In these ESMs, effects of temperature and precipitation on
290 SOC stocks are driven by soil respiration. Most current ESMs simulate the response of soil
291 respiration to temperature using either a Q_{10} or Arrhenius equation (Wynn et al., 2006), such that
292 a higher temperature causes more soil respiration, and, all else equal, eventually reduces SOC
293 stocks (Figure 5b). Our results showed diverse control of precipitation on SOC stocks in
294 different ESMs. Todd-Brown et al. (2013) showed that ESM soil respiration either increases
295 monotonically with precipitation, or first increases to a plateau under optimal precipitation and
296 then decreases with further increasing precipitation. Consistent with those results, the ESMs we
297 analyzed in this study showed different dependence of SOC storage on annual precipitation.

298 In this study, we found that, in comparison to the patterns that emerged from
299 observations, ESMs have distinctively different emergent relationships between environmental
300 factors and SOC stocks. These results could either result from unrealistic parameterization or
301 missing critical processes in model representation. Our results show that observed global SOC
302 stocks are controlled not only by temperature, precipitation, and NPP. Effects of other
303 environmental factors, such as drought severity index and cation exchange capacity should also
304 be considered in future representations of SOC dynamics in ESMs. It is also imperative to
305 compare observational data and ESM simulations to improve model structures and
306 parameterization.



307

308

309 **5. Conclusion**

310 Our results document disagreement between environmental controllers of SOC stocks in
311 observations and ESM land models. Specifically, NPP, annual temperature, and annual
312 precipitation have dominant control in modeled SOC stocks. In contrast, diurnal temperature,
313 drought index, annual temperature, cation exchange capacity, and other soil related variables are
314 the dominant controllers of observed SOC stocks. Using field observations and data for
315 environmental factors, machine learning techniques predict about 60% of the variability in
316 observed global SOC stocks, while in ESMs, only a few environmental factors predict about
317 95% of the variability in predicted SOC stocks. Comparisons of derived functional relationships
318 between the environmental factors and SOC stocks in observations and ESM models also show
319 discrepancies. These discrepancies indicate the importance of efforts to benchmark ESM land
320 models and to improve the mechanistic representations that are affected by the observed
321 dominant environmental controllers. Such an effort could decrease disagreements between
322 observed and modeled SOC stocks.

323

324 **Acknowledgements**

325 This study was supported jointly by the Laboratory Directed Research and Development
326 program of Sandia National Laboratories and the Reducing Uncertainties in Biogeochemical
327 Interactions through Synthesis and Computation Science Focus Area (RUBISCO SFA), which is
328 sponsored by the Regional and Global Model Analysis (RGMA) activity of the Earth
329 Environmental Systems Modeling (EESM) Program in the Earth and Environmental Systems



330 Sciences Division (EESD) of the Office of Biological and Environmental Research (BER) in
331 the US Department of Energy Office of Science. Sandia National Laboratories is a multimission
332 laboratory managed and operated by National Technology and Engineering Solutions of Sandia,
333 LLC, a wholly owned subsidiary of Honeywell International, Inc., for the U.S. Department of
334 Energy's National Nuclear Security Administration under contract DE-NA-0003525. Lawrence
335 Berkeley National Laboratory (LBNL) is managed by the Regents of the University of California
336 for the U.S. Department of Energy under Contract No. DE-AC02-05CH11231. Oak Ridge
337 National Laboratory (ORNL) is managed by UT-Battelle, LLC, for the U.S. Department of
338 Energy under Contract No. DE-AC05-00OR22725.

339 **References**

- 340
341 Anderegg, W. R. L., Berry, J. A., Smith, D. D., Sperry, J. S., Anderegg, L. D. L., and Field, C.
342 B.: The roles of hydraulic and carbon stress in a widespread climate-induced forest die-off, *Proc*
343 *Natl Acad Sci U S A*, 109, 233–237, <https://doi.org/10.1073/PNAS.1107891109>, 2012.
344
345 Arnold, D., Wagner, P., and Baayen, R. B.: Using generalized additive models and random
346 forests to model prosodic prominence in German, *isca-speech.org*, 2013.
347
348 Arora, V., Katavouta, A., Williams, R., Jones, C. D., Brovkin, V., Friedlingstein, P., Schwinger,
349 J., Bopp, L., Boucher, O., Cadule, P., Chamberlain, M., Christian, J., Delire, C., Fisher, R.,
350 Hajima, T., Ilyina, T., Joetzjer, E., Kawamiya, M., Koven, C., Krasting, J., Law, R., Lawrence,
351 D., Lenton, A., Lindsay, K., Pongratz, J., Raddatz, T., Séférian, R., Tachiiri, K., Tjiputra, J.,
352 Wiltshire, A., Wu, T., and Ziehn, T.: Carbon–concentration and carbon–climate feedbacks in
353 CMIP6 models and their comparison to CMIP5 models, *Biogeosciences*, 17, 4173–4222,
354 <https://doi.org/10.5194/bg-17-4173-2020>, 2020.
355
356 Azizi-Rad, M., Guggenberger, G., Ma, Y., and Sierra, C. A.: Sensitivity of soil respiration rate
357 with respect to temperature, moisture and oxygen under freezing and thawing, *Soil Biology and*
358 *Biochemistry*, 165, <https://doi.org/10.1016/j.soilbio.2021.108488>, 2022.
359
360 Batjes, N., Ribeiro E., and Oostrum, A.: Standardised soil profile data to support global mapping
361 and modelling (WoSIS snapshot 2019), *Earth Syst. Sci. Data*, 12, 299–320,
362 <https://doi.org/10.5194/essd-12-299-2020>, 2020.
363



- 364 Breiman, L.: Random forests, *Mach Learn*, 45, 5–32, <https://doi.org/10.1023/A:1010933404324>,
365 2001.
366
- 367 Chagas, C. da S., Junior, W de C., Bhering, S. B., and Filho, B. C.: Spatial prediction of soil
368 surface texture in a semiarid region using random forest and multiple linear regressions, *Catena*,
369 139, 232–240, <https://doi.org/10.1016/j.catena.2016.01.001>, 2016.
370
- 371 Chen, S., Wang, W., Xu, W., Wang, Y., Wan, H., Chen, D., Tang, Z., Tang, X., Zhou, G., Xie,
372 Z., Zhou, D., Shangguan, Z., Huang, J., He, J. S., Wang, Y., Sheng, J., Tang, L., Li, X., Dong,
373 M., Wu, Y., Wang, Q., Wang, Z., Wu, J., Stuart Chapin, F., and Bai, Y.: Plant diversity enhances
374 productivity and soil carbon storage, *Proc Natl Acad Sci U S A*, 115, 4027–4032,
375 <https://doi.org/10.1073/PNAS.1700298114>, 2018.
376
- 377 Collier, N., Hoffman, F. M., Lawrence, D. M., Keppel-Aleks, G., Koven, C. D., Riley, W. J.,
378 Mu, M., and Randerson, J. T.: The International Land Model Benchmarking (ILAMB) system:
379 design, theory, and implementation, *Wiley Online Library*, 10, 2731–2754,
380 <https://doi.org/10.1029/2018MS001354>, 2018.
381
- 382 Frank, S., Schmid, E., Havlík, P., Schneider, U.A., Böttcher, H., Balkovič, J. and Obersteiner,
383 M.: The dynamic soil organic carbon mitigation potential of European cropland, *Global*
384 *Environmental Change*, 35, 269–278, <https://doi.org/10.1016/j.gloenvcha.2015.08.004>, 2015.
385
- 386 Friedlingstein, P., Meinshausen, M., Arora, V.K., Jones, C.D., Anav, A., Liddicoat, S.K. and
387 Knutti, R.: Uncertainties in CMIP5 climate projections due to carbon cycle feedbacks, *Journal of*
388 *Climate*, 27, 511–526, <https://doi.org/10.1175/JCLI-D-12-00579.1>, 2014.
389
- 390 Georgiou, K., Malhotra, A., Wieder, W. R., Ennis, J. H., Hartman, M. D., Sulman, B. N., Berhe,
391 A. A., Grandy, A. S., Kyker-Snowman, E., Lajtha, K., Moore, J. A. M., Pierson, D., and Jackson,
392 R. B.: Divergent controls of soil organic carbon between observations and process-based models,
393 *Biogeochemistry*, 156, 5–17, <https://doi.org/10.1007/S10533-021-00819-2>, 2021.
394
- 395 Hastie, T. and Tibshirani, R.: Generalized additive models: Some applications, *J Am Stat Assoc*,
396 82, 371–386, <https://doi.org/10.1080/01621459.1987.10478440>, 1987.
397
- 398 Hinge, G., Surampalli, R. Y., and Goyal, M. K.: Prediction of soil organic carbon stock using
399 digital mapping approach in humid India, *Environ Earth Sci*, 77, [https://doi.org/10.1007/S12665-](https://doi.org/10.1007/S12665-018-7374-X)
400 018-7374-X, 2018.
401
- 402 Hurrell, J.W., Holland, M.M., Gent, P.R., Ghan, S., Kay, J.E., Kushner, P.J., Lamarque, J.F.,
403 Large, W.G., Lawrence, D., Lindsay, K. and Lipscomb, W.H.: The community earth system
404 model: a framework for collaborative research, *Bulletin of the American Meteorological Society*,
405 94, 1339–1360, <https://doi.org/10.1175/BAMS-D-12-00121.1>, 2013.
406
- 407 Jiang, H., Deng, Q., Zhou, G., Hui, D., Zhang, D., Liu, S., Chu, G., and Li, J.: Responses of soil
408 respiration and its temperature/moisture sensitivity to precipitation in three subtropical forests in
409 southern China, *Biogeosciences*, 10, 3963–3982, <https://doi.org/10.5194/bg-10-3963-2013>, 2013.



- 410
411 Lal, R.: Soil health and carbon management, *Food Energy Secur*, 5, 212–222,
412 <https://doi.org/10.1002/fes3.96>, 2016.
413
414 Lal, R.: Managing soils for negative feedback to climate change and positive impact on food and
415 nutritional security, *Soil Sci Plant Nutr*, 66, 1–9,
416 <https://doi.org/10.1080/00380768.2020.1718548>, 2020.
417
418 Lauer, A., Eyring, V., Righi, M., Buchwitz, M., Defourny, P., Evaldsson, M., Friedlingstein, P.,
419 de Jeu, R., de Leeuw, G., Loew, A. and Merchant, C.J.: Benchmarking CMIP5 models with a
420 subset of ESA CCI Phase 2 data using the ESMValTool, *Remote Sensing of Environment*, 203,
421 9–39, <https://doi.org/10.1016/j.rse.2017.01.007>, 2017.
422
423 Li, S., Liu, Y., Lyu, S., Wang, S., Pan, Y., and Qin, Y.: Change in soil organic carbon and its
424 climate drivers over the Tibetan Plateau in CMIP5 earth system models, *Theor Appl Climatol*,
425 145, 187–196, <https://doi.org/10.1007/S00704-021-03631-Y>, 2021.
426
427 Loveland, T. R. and Belward, A. S.: The igbp-dis global 1km land cover data set, discover: First
428 results, *Int J Remote Sens*, 18, 3289–3295, <https://doi.org/10.1080/014311697217099>, 1997.
429
430 Luo, Y. Q., Randerson, J., Abramowitz, G., Bacour, C., Blyth, E., Carvalhais, N., Ciais, P.,
431 Dalmonech, D., Fisher, J., Fisher, R., Friedlingstein, P., Hibbard, K., Hoffman, F., Huntzinger,
432 D., Jones, C. D., Koven, C., Lawrence, D., Li, D. J., Mahecha, M., Niu, S. L., Norby, R., Piao, S.
433 L., Qi, X., Peylin, P., Prentice, I. C., Riley, W., Reichstein, M., Schwalm, C., Wang, Y. P., Xia,
434 J. Y., Zaehle, S., and Zhou, X. H.: A framework for benchmarking land models,
435 *bg.copernicus.org*, 9, 1899–1944, <https://doi.org/10.5194/bg-9-1899-2012>, 2012.
436
437 Luo, Z., Viscarra-Rossel, R.A. and Qian, T.: Similar importance of edaphic and climatic factors
438 for controlling soil organic carbon stocks of the world, *Biogeosciences*, 18, 2063–2073.,
439 <https://doi.org/10.5194/bg-18-2063-2021>, 2021.
440
441 McBratney, A.B., Santos, M.M. and Minasny, B.: On digital soil mapping, *Geoderma*, 117, 3–52,
442 [https://doi.org/10.1016/S0016-7061\(03\)00223-4](https://doi.org/10.1016/S0016-7061(03)00223-4), 2003.
443
444 Mekonnen, Z., Riley, W., ... J. R.-E., and 2022, undefined: Wildfire exacerbates high-latitude
445 soil carbon losses from climate warming, *iopscience.iop.org*, [https://doi.org/10.1088/1748-](https://doi.org/10.1088/1748-9326/ac8be6)
446 [9326/ac8be6](https://doi.org/10.1088/1748-9326/ac8be6), 2022.
447
448 Mishra, U., Gautam, S., Riley, W. J., and Hoffman, F. M.: Ensemble Machine Learning
449 Approach Improves Predicted Spatial Variation of Surface Soil Organic Carbon Stocks in Data-
450 Limited Northern Circumpolar Region, *Front Big Data*, 3,
451 <https://doi.org/10.3389/FDATA.2020.528441/FULL>, 2020.
452
453 Mishra, U., Yeo, K., Adhikari, K., Riley, W. J., Hoffman, F. M., Hudson, C., and Gautam, S.:
454 Empirical relationships between environmental factors and soil organic carbon produce



- 455 comparable prediction accuracy to machine learning, Wiley Online Library, 86, 1611–1624,
456 <https://doi.org/10.1002/saj2.20453>, 2022.
457
- 458 O'Brien, S.L., Jastrow, J.D., Grimley, D.A. and Gonzalez-Meler, M.A.: Edaphic controls on soil
459 organic carbon stocks in restored grasslands, *Geoderma*, 251, 117-123,
460 <https://doi.org/10.1016/j.geoderma.2015.03.023>, 2015.
461
- 462 Sellar, A. A., Jones, C. G., Mulcahy, J. P., Tang, Y., Yool, A., Wiltshire, A., O'Connor, F. M.,
463 Stringer, M., Hill, R., Palmieri, J., Woodward, S., de Mora, L., Kuhlbrodt, T., Rumbold, S. T.,
464 Kelley, D. I., Ellis, R., Johnson, C. E., Walton, J., Abraham, N. L., Andrews, M. B., Andrews,
465 T., Archibald, A. T., Berthou, S., Burke, E., Blockley, E., Carslaw, K., Dalvi, M., Edwards, J.,
466 Folberth, G. A., Gedney, N., Griffiths, P. T., Harper, A. B., Hendry, M. A., Hewitt, A. J.,
467 Johnson, B., Jones, A., Jones, C. D., Keeble, J., Liddicoat, S., Morgenstern, O., Parker, R. J.,
468 Predoi, V., Robertson, E., Siahhaan, A., Smith, R. S., Swaminathan, R., Woodhouse, M. T., Zeng,
469 G., and Zerroukat, M.: UKESM1: Description and Evaluation of the U.K. Earth System Model, *J*
470 *Adv Model Earth Syst*, 11, 4513–4558, <https://doi.org/10.1029/2019MS001739>, 2019.
471
- 472 Shi, X., Mao, J., Thornton, P.E. and Huang, M.: Spatiotemporal patterns of evapotranspiration in
473 response to multiple environmental factors simulated by the Community Land Model,
474 *Environmental Research Letters*, 8, 024012, <https://doi.org/10.1088/1748-9326/8/2/024012>,
475 2013.
476
- 477 Solly, E. F., Weber, V., Zimmermann, S., Walthert, L., Hagedorn, F., and Schmidt, M. W. I.: A
478 Critical Evaluation of the Relationship Between the Effective Cation Exchange Capacity and
479 Soil Organic Carbon Content in Swiss Forest Soils, *Frontiers in Forests and Global Change*, 3,
480 <https://doi.org/10.3389/FFGC.2020.00098/FULL>, 2020.
481
- 482 Sreenivas, K., Dadhwal, V.K., Kumar, S., Harsha, G.S., Mitran, T., Sujatha, G., Suresh, G.J.R.,
483 Fyzee, M.A. and Ravisankar, T.: Digital mapping of soil organic and inorganic carbon status in
484 India, *Geoderma*, 269, 160-173, <https://doi.org/10.1016/j.geoderma.2016.02.002> , 2016.
485
- 486 Sun, Y., Piao, S., Huang, M., Ciais, P., Zeng, Z., Cheng, L., Li, X., Zhang, X., Mao, J., Peng, S.,
487 Poulter, B., Shi, X., Wang, X., Wang, Y. P., and Zeng, H.: Global patterns and climate drivers of
488 water-use efficiency in terrestrial ecosystems deduced from satellite-based datasets and carbon
489 cycle models, *Global Ecology and Biogeography*, 25, 311–323,
490 <https://doi.org/10.1111/GEB.12411>, 2016.
491
- 492 Todd-Brown, K. E. O., Randerson, J. T., Post, W. M., Hoffman, F. M., Tarnocai, C., Schuur, E.
493 A. G., and Allison, S. D.: Causes of variation in soil carbon simulations from CMIP5 Earth
494 system models and comparison with observations, *Biogeosciences*, 10, 1717–1736,
495 <https://doi.org/10.5194/BG-10-1717-2013>, 2013.
496
- 497 Wiesmeier, M., Barthold, F., Blank, B., and Kögel-Knabner, I.: Digital mapping of soil organic
498 matter stocks using Random Forest modeling in a semi-arid steppe ecosystem, *Plant Soil*, 340,
499 7–24, <https://doi.org/10.1007/S11104-010-0425-Z>, 2011.
500



- 501 Wiesmeier, M., Barthold, F., Spörlein, P., Geuß, U., Hangen, E., Reischl, A., Schilling, B.,
502 Angst, G., von Lützow, M. and Kögel-Knabner, I.: Estimation of total organic carbon storage
503 and its driving factors in soils of Bavaria (southeast Germany), *Geoderma Regional*, 1, 67-78,
504 <https://doi.org/10.1016/j.geodrs.2014.09.001>, 2014.
505
506 Wynn, J. G., Bird, M. I., Vellen, L., Grand-Clement, E., Carter, J., and Berry, S. L.: Continental-
507 scale measurement of the soil organic carbon pool with climatic, edaphic, and biotic controls,
508 *Wiley Online Library*, 20, <https://doi.org/10.1029/2005GB002576>, 2006.
509
510 Xiao-Ge, X.I.N., Tong-Wen, W.U., Jie ZHANG, F.Z., Wei-Ping, L.I., Yan-Wu ZHANG,
511 Y.X.L., Yong-Jie, F.A.N.G., Wei-Hua, J.I.E., Li ZHANG, M.D., Xue-Li, S.H.I., Jiang-Long, L.I.
512 and Min, C.H.U.: Introduction of BCC models and its participation in CMIP6, *Advances in*
513 *Climate Change Research*, 15, 533, <https://doi.org/10.12006/j.issn.1673-1719.2019.039>, 2019.
514
515 Yigini, Y., Olmedo, G., Reiter, S., Baritz, R., and Viatkin, K.: *Soil organic carbon mapping:*
516 *cookbook*, 2018.
517



Figures and Tables

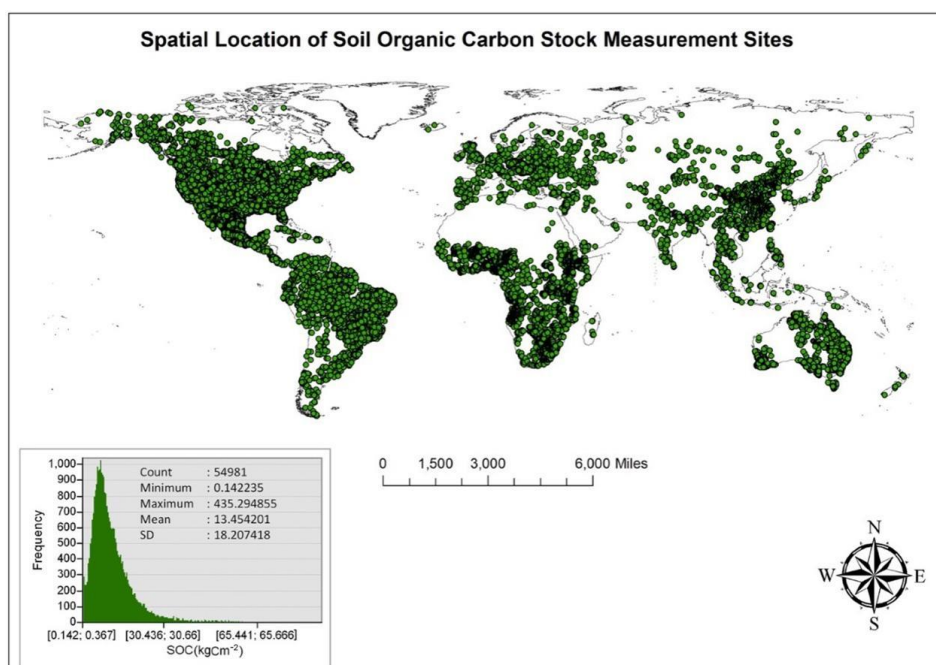


Figure 1. Spatial and statistical distributions of 54,000 soil organic carbon profiles used in this study.

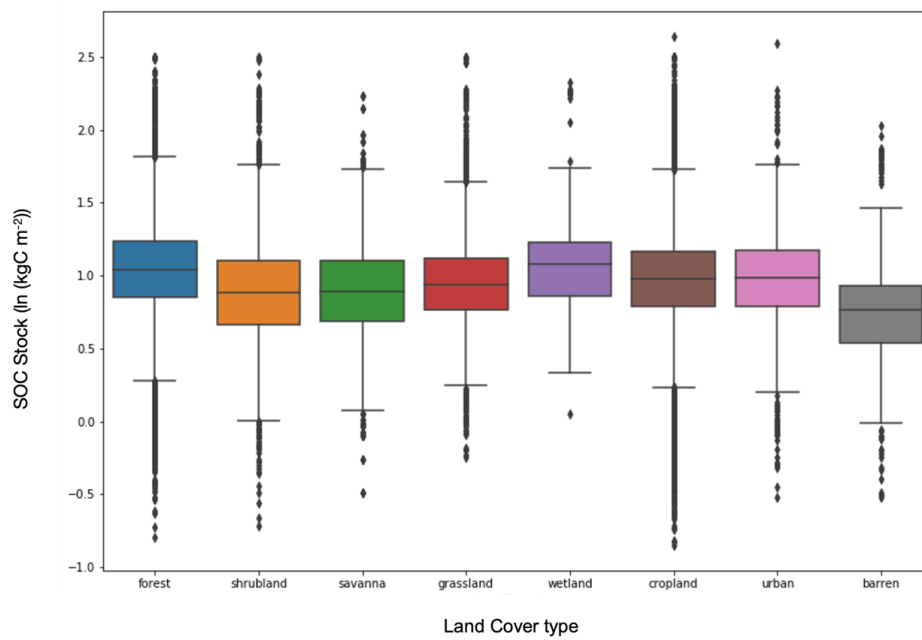


Figure 2: Boxplot of soil organic carbon content (logarithmic scale) for each biome or land cover type analyzed in this study. The horizontal line in the middle of the boxes is the median while their lower and upper limits correspond to the first and third quartiles.

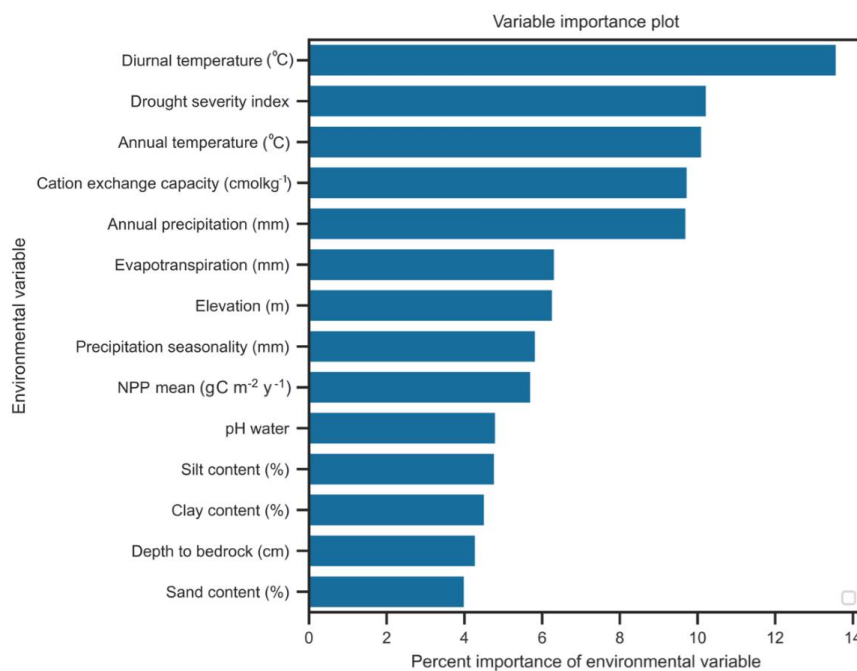


Figure 3: Importance of different environmental factors to predict the global soil organic carbon stocks in observations.

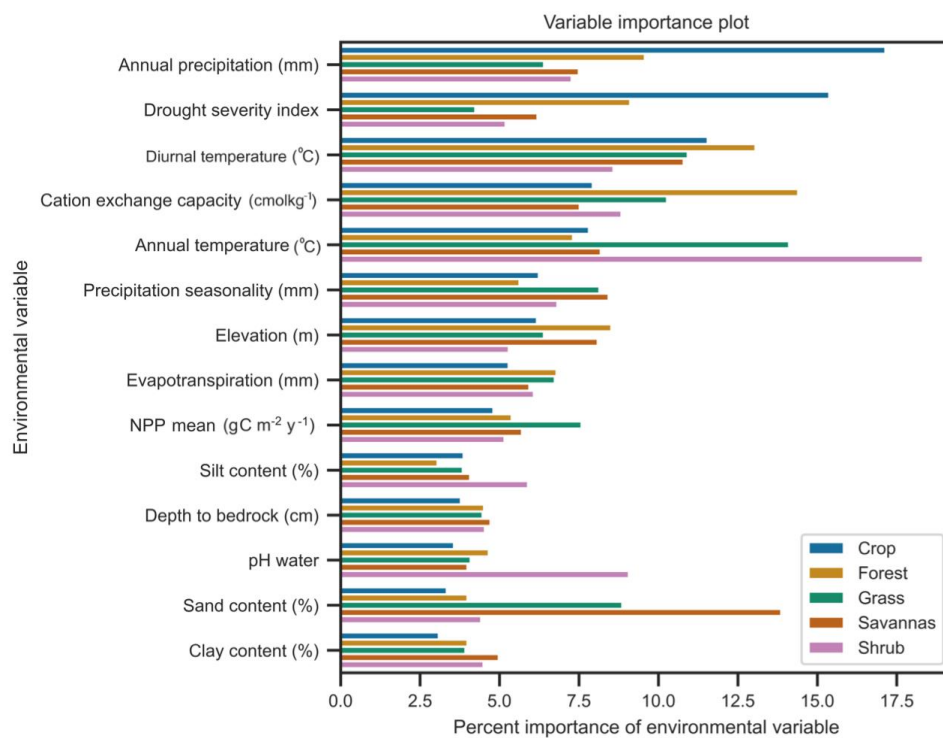


Figure 4: Strengths and importance of environmental controllers of observed SOC stocks within different biomes.

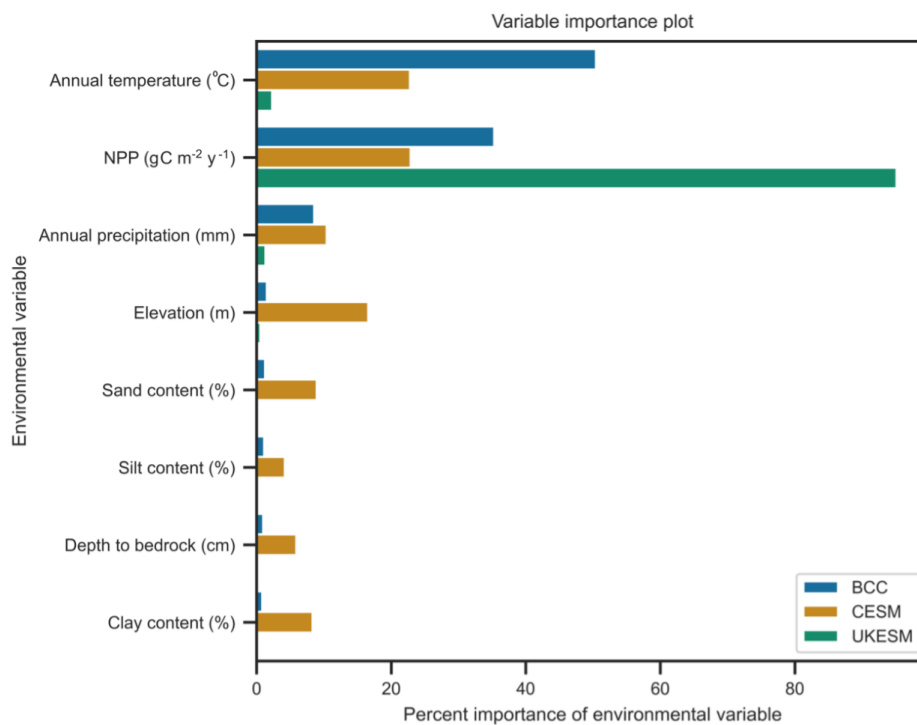


Figure 5: Importance of different environmental factors on global soil organic carbon stocks in three CMIP6 earth system models.

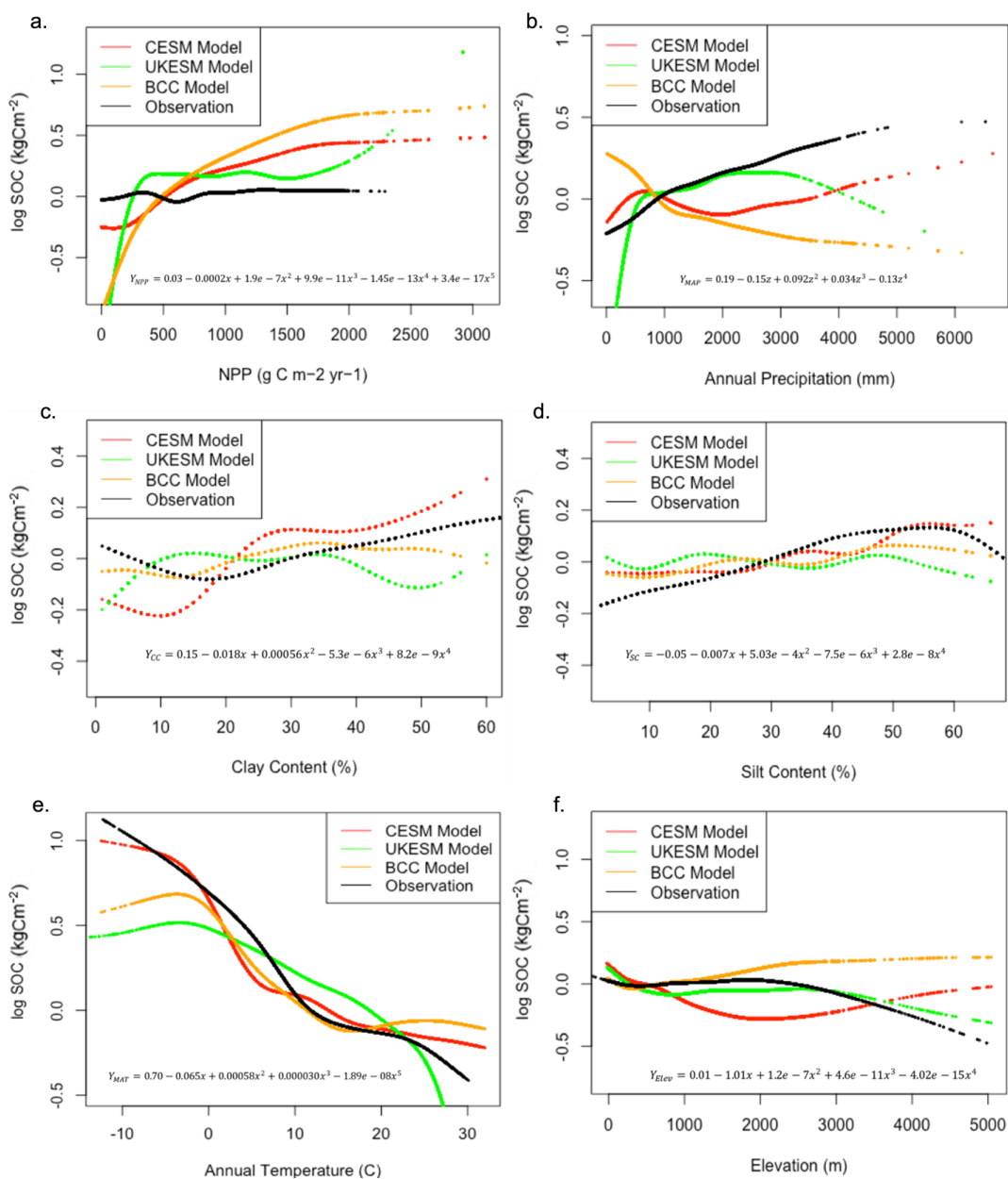


Figure 6: Predictive relationships between environmental factors and soil organic carbon stocks in observations (black line) and CMIP6 earth system models (different colors).



Table 1: Descriptive statistics of global soil organic carbon stocks at 0-100 cm depth interval.

Location	Depth (cm)	Minimum (kgC m ⁻²)	Maximum (kgC m ⁻²)	Mean (kgC m ⁻²)	Median (kgC m ⁻²)	Standard Deviation (kgC m ⁻²)
Global	0-100	0.14	435.3	13.5	9.5	18.2
Cropland	0-100	0.14	435.3	12.75	9.5	16.0
Grassland	0-100	0.56	315.9	12.1	8.7	16.8
Forest	0-100	0.16	314.4	15.9	10.9	20.7
Shrubland	0-100	0.19	312.5	13.6	7.6	25.6
Savannas	0-100	0.32	309.1	12.6	9.2	15.2



Table 2: Prediction accuracies of Random Forest models across biomes and at global scale in predicting SOC stocks.

Location	Depth (cm)	R square (RF)	RMSE
Global	0-100	0.61	0.46
Cropland	0-100	0.65	0.51
Grassland	0-100	0.57	0.46
Forest	0-100	0.59	0.52
Shrubland	0-100	0.64	0.54
Savannas	0-100	0.48	0.52